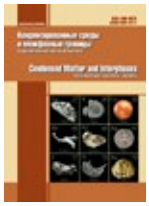

ISSN 1606-867X (Print)
ISSN 2687-0711 (Online)
Condensed Matter and Interphases
Kondensirovannye Sredy i Mezhfaznye Granitsy
https://journals.vsu.ru/kcmf/

**Original articles**

Research article
https://doi.org/10.17308/kcmf.2024.26/12082

# Photoelectrochemical activity of oxide films on silver-palladium alloys in an alkaline solution

**I. A. Belyanskaya, M. Yu. Bocharnikova, M. M. Murtazin, S. N. Grushevskaya✉, O. A. Kozaderov, A. V. Vvedensky**

*Voronezh State University,*
*1 Universitetskaya pl., Voronezh 394018, Russian Federation*

**Abstract**

The continuously increasing energy needs of humanity are causing a number of serious environmental problems. One of the methods for the solution of such problems is the photocatalytic or photoelectrochemical production of a fairly environmentally friendly fuel - hydrogen gas. The studies in this field are mainly associated with the search for semiconductor material that is most suitable for photocatalysis. Oxides of some metals, including silver, can be used as such a material. The photocatalytic or photoelectrochemical activity of the oxide is determined by the features of its electronic structure and can increase significantly when combined with another oxide. Therefore, anodic oxidation of binary alloys is considered as an accessible and, most importantly, controlled method for combining oxides of various metals. The aim of this study was to reveal the role of alloying of silver with palladium in the photoelectrochemical activity of oxide films anodicly formed in deaerated 0.1 M KOH.

The anodic formation of oxide films was carried out by the potentiodynamic method in an alkaline medium on silver and its alloys with palladium, the concentration of which ranged from 5 to 30 at. %. Photoelectrochemical activity was assessed by the magnitude of the photocurrent generated in the oxide film directly during its formation and subsequent reduction. The photocurrent was measured in a pulsed lighting mode of the electrode surface with a quasimonochromatic LED with a wavelength of 470 nm.

A positive photocurrent was recorded on all studied samples, which indicates the predominance of donor structural defects in the forming oxide film. With an increase in the concentration of palladium in the alloy, the range of potentials of photoelectrochemical activity of formed anodicly oxide films expanded. The maximum photocurrent achieved during the anodic potentiodynamic formation of the oxide film was higher, the lower the palladium concentration was. During the cathodic potentiodynamic reduction of the formed oxide films, it was possible to record even higher values of photocurrents than during their anodic formation. The highest photoelectrochemical activity, characterized by a photocurrent density of 2.89 μA/cm$^2$ and incidental proton-to-electron conversion efficiency of 7.6%, was observed in the oxide film anodically formed on silver by the time the potential reached 0.6 V. Comparable values of the photocurrent and quantum efficiency (2.12 μA/cm$^2$ and 5.6%) were recorded in the oxide film on the alloy with a palladium concentration of 10 at. % during its potentiodynamic reduction.

**Keywords:** Silver-palladium alloys, Anodic oxide formation, Photoelectrochemical activity, Photocurrent, Cyclic voltammetry

***Funding:*** The study was supported by the Ministry of Science and Higher Education of the Russian Federation within the framework of state order to higher education institutions in the sphere of scientific research for 2022–2024, project No. FZGU-2022-0003.

***Acknowledgements:*** The authors are grateful to the Centre for collective use of scientific equipment of Voronezh State University – Agapov B. L. for performing energy-dispersive microanalysis and Kannykin S. V. for performing X-ray diffractometry.

***For citation:*** Belyanskaya I. A., Bocharnikova M. Y., Murtazin M. M., Grushevskaya S. N., Kozaderov O. A., Vvedenskii A. V. Photoelectrochemical activity of oxide films on silver-palladium alloys in alkaline solution. *Condensed Matter and Interphases*. 2024;26(2): 213–224. https://doi.org/10.17308/kcmf.2024.26/12082

✉ Svetlana N. Grushevskaya, e-mail: sg@chem.vsu.ru

***Для цитирования:*** Белянская И. А., Бочарникова М. Ю., Муртазин М. М., Грушевская С. Н., Козадеров О. А., Введенский А. В. Фотоэлектрохимическая активность оксидных пленок на серебряно-палладиевых сплавах в щелочном растворе. *Конденсированные среды и межфазные границы*. 2024;26(2): 213–224. https://doi.org/10.17308/kcmf.2024.26/12082

## 1. Introduction

Semiconductors based on metal oxides are used in modern technologies of opto- and microelectronics (including complementary metal-oxide-semiconductor structures), electrocatalysis, the manufacture of sensor and current-generating devices, as well as photocatalytic and photoelectrochemical hydrogen production [1–3]. Such technologies for production of hydrogen have been particularly intensively developed in recent decades, as they allow solving problems with continuously increasing energy needs by humanity in a fairly environmentally friendly way.

In both photocatalytic and photoelectrochemical processes the first stage is the illumination of the semiconductor material and the generation of electron-hole pairs [4–7]. At the next stage the charge carriers are separated in space, migrate to the interfaces and pass into the electrolyte. In the case of photocatalysis, photoinduced electrons and holes participate in reduction and oxidation processes occurring at the semiconductor/electrolyte interfaces [6]. In the case of photoelectrocatalysis, the reduction or oxidation process occurs at the semiconductor photoelectrode/electrolyte interface, and charge carriers move from one electrode to the second via the external circuit [7]. Due to the presence of similar steps, there is usually a correlation between the rate of the photocatalytic reaction and the photocurrent density [8, 9]. Thus, photocatalytic activity of semiconductor materials can be assessed based on the values of the photocurrent generated under illumination [9].

The efficiency of the processes of photocatalysis and photoelectrolysis is determined by the characteristics of the electronic structure of the semiconductor material and depends on the method of its preparation. The anodic oxidation of metals and alloys is one of the methods of the production of oxide films with controlled properties. The oxidation of alloys allow to synthesize oxide structures with complex chemical composition [2, 3], which can lead to an increase in their photoelectrochemical activity [10].

Silver-based alloys, during anodic oxidation of which silver oxides are predominantly formed were considered as a model system in this study. Oxide Ag(I) is a narrow-bandgap semiconductor, used in electronics industry for the production of electrical, optical and magneto-optical data storage devices [11–13], for the manufacture of solar cells and photovoltaic devices [14]. In addition, $Ag_2O$ nanoparticles are used as catalysts [15], and high photocatalytic activity of the $Ag_2O$/AgO redox pair in relation to the oxygen evolution reaction was demonstrated [16] . Catalysts based on silver and its oxides are promising materials for photocatalytic and photoelectrocatalytic decomposition of water [17, 18]. The effect of alloy formation on the properties of anodicly formed silver oxides has not been studied properly.

In [19–21], this effect was studied using the alloys of silver with gold containing 1, 4 and 15 at. %. The objects of study were obtained by smelting. During potentiostatic anodic oxidation in a deaerated 0.1 M KOH solution, silver (I) oxide was formed on their surface, while gold remained thermodynamically stable. The photoelectrochemical properties of the formed oxide were studied by measuring the photocurrent as the deviation of the dark current during pulsed lighting mode of the electrode surface with a LED with a wavelength of 470 nm and an irradiation power of $3.6 \cdot 10^{15}$ photon/cm$^2$s. This method allows the characterization of the oxide directly during its formation. It has been established that the photocurrent density, and hence the photoelectrochemical activity in $Ag_2O$ silver oxides of n-type formed anodicly on silver-gold alloys decreased sharply with increase in gold concentration. The maximum photoelectrochemical activity was recorded in Ag(I) oxide potentiostatically formed on silver. Silver oxides $Ag_2O$ and AgO, anodically formed on silver-zinc alloys, were investigated using the same methods in [22, 23]. The presence of up to 30 at. % of zinc in the alloy allows the presence

of a small amount of zinc oxide in the oxide film. However, an increase in the photocurrent due to the combination of these oxides was not observed. On the contrary, the photoelectrochemical activity of formed anodicly oxide films slightly decreased with increased zinc concentration in the alloy.

In this study, palladium, with widely known catalytic and photocatalytic properties [24, 25], is considered as the second component of silver-based alloys. In alkaline solutions, palladium can oxidize and as the result its surface is being covered with an oxide film. Palladium oxide PdO is a p-type semiconductor [26] with a wide range of technological applications, including sensor production [26–28], catalysis [29, 30], photocatalysis and photoelectrolysis [31–33]. It was reported [29, 33] that doping with PdO oxide increases the photoelectrochemical activity of various oxides of other metals. Thin films $Ag_{1-x}Pd_x$ ($0 \leqslant x \leqslant 1$) with a thickness of ~70 nm were synthesized using the vapor deposition method in [34]. Using cyclic voltammetry in an alkaline solution, it was shown that the catalytic activity for the oxygen evolution reaction increases up to 5 times compared to pure palladium. In [35], homogeneous nanoparticles of Ag–Pd alloys with a size of about 5 nm were obtained by the thermolysis of precursors. According to cyclic voltammetry and measurements of the amount of removed CO, it was shown that the activity of the alloys in relation to the oxygen evolution reaction was higher than the activity of pure components. Moreover, the experimentally measured activity was higher than that calculated based on the assumption about linear combination of the properties of the individual components. The activity of $AgPd_2$ alloy was by 60% higher than that of pure palladium, and for $Ag_4Pd$ alloy activity was 3.2 times higher than calculated by the linear combination method. Similar trends are observed for other alloys with a high silver content: it was higher for $Ag_9Pd$ by 2.7 times and for $Ag_2Pd$ by 2.3 times. The synergistic effect was associated with the special arrangement of the atoms of the individual components [35] – single palladium atoms were surrounded by silver atoms.

Taking into account the high catalytic activity of silver alloys with palladium described in the literature, it can be assumed that the photoelectrochemical activity of oxides formed anodicly on such alloys will increase in comparison with Ag(I) oxide formed on silver. The aim of this study was to reveal the role of formation of silver and palladium alloys in the photoelectrochemical activity of oxide films formed anodicly in deaerated 0.1 M KOH. In contrast to the potentiostatic conditions of anodic oxidation considered in [19–23], stepwise polarization mode of electrodes for the detection of the potential region of the highest photocurrent values, and therefore the photoelectrochemical activity of the forming anodic films was used in this study.

## 2. Experimental

### *2.1. Materials and methods*

Oxide films formed during the electrochemical oxidation of silver and silver alloys with palladium in a deaerated solution of 0.1 M KOH were used as objects of the study.

The alloys were obtained from silver and palladium with a purity of 99.99 mass. % by heating for two hours in evacuated ampoules at a temperature above the liquidus line. Slow cooling to room temperature was carried out in a closed oven. Calculated palladium concentration in samples $X_{Pd}$ was 5, 10, 15, 20, and 30 at. %. These values will be used further in the text. The elemental composition of the resulting alloys was determined using energy dispersive X-ray analysis carried out using a JSM-6380LV JEOL scanning electron microscope with an INCA 250 microanalysis system*. Phase composition of alloys was studied using ARL X'TRA X-ray diffractometer*.

One cylindrical sample was made from each alloy. All samples are equipped with a current lead and reinforced with polymerized epoxy resin in such a way that the end surface remained open for access to the solution. The average geometric surface area was 0.59±0.02 $cm^2$.

A working solution of 0.1 M KOH was prepared from a chemically pure reagent and bidistilled water, deaerated with chemically pure argon.

* The results of the research were obtained using the Centre for the Collective Use of Scientific Equipment of Voronezh State University. URL: https://ckp.vsu.ru

### *2.2. Photoelectrochemical studies*

Photoelectrochemical studies were carried out in a plexiglass cell with undivided anode and cathode spaces. The cell was protected from electromagnetic interference by a metal shield. The bottom of the cell was equipped with a quartz window for illumination of the horizontally oriented surface of the working electrode. The auxiliary electrode was a platinum wire, the reference electrode was silver oxide, prepared by the electrochemical oxidation of a silver plate at a current of 5 mA for 20 min in aerated 0.1 M KOH. The potential of such an electrode was 0.428 V relative to a standard hydrogen electrode. The potentials in the study are presented relative to the standard hydrogen electrode.

Before each measurement, the surface of the working electrode, made of silver or a silver-palladium alloy, was subjected to striping on sanding paper with decreasing grain size (P800, P1500 and P2500), and then polishing on chamois. The polished surface was degreased with isopropyl alcohol. This preparation was followed by a 5-minute cathodic standardization of the surface in a working solution at a potential of $E_c$ = –0.3 V. This potential value was below the equilibrium potentials of formation/reduction of both silver (0.41 V) and palladium (0.07 V) oxides. At the same time, it was noticeably higher than the equilibrium potential of the hydrogen electrode in 0.1 M KOH with pH 12.89 (–0.76 V), which excluded the possibility of hydrogen incorporation into the electrode material.

The potential region for the formation of oxide films was determined by cyclic voltammetry. The potential was scanned with rate of 5 mV/s from $E_c$ in the anodic direction until appearance of maximum current, presumably associated with the formation of Ag(I) oxide. After this, scanning was carried out at the same rate until the value $E_c$.

The photoelectrochemical activity of formed anodicly oxides was assessed based on the photocurrent value, determined as the difference between the current under illumination and the current in the absence of illumination. Illumination was carried out in pulsed mode with a quasimonochromatic emitting LED (Table 1).

The incidental proton-to-electron conversion efficiency (IPCE) was calculated using the equation [36]:

$$IPCE\ (\%) = 100\% \cdot 1240 \cdot i_{ph} / (\lambda \cdot P),$$

Where $i_{ph}$ – photocurrent density (mA/cm$^2$), λ – wavelength (nm), $P$ – lighting power (mW/cm$^2$).

To determine the potential range and level of photoelectrochemical activity of silver oxide, a stepwise polarization mode of the electrodes was carried out (Fig. 1). After cathodic preparation of the electrode surface at $E_c$ the potential was switched to the initial value $E_i$ = 0.48 V. In preliminary experiments we established that below this value the photocurrent does not occur. From $E_i$ value the potential increased every 5 min by 20 mV with continuous recording of the polarization current and photocurrent in a pulsed lighting mode of the electrode surface. After the maximum current in the voltammogram associated with the formation of silver oxide, the potential decreased with the same step until full disappearance of the photocurrent. The polarization current and photocurrent densities were calculated per the geometric surface area of the working electrodes.

Electrochemical and photoelectrochemical studies were carried out using a Compact-2015

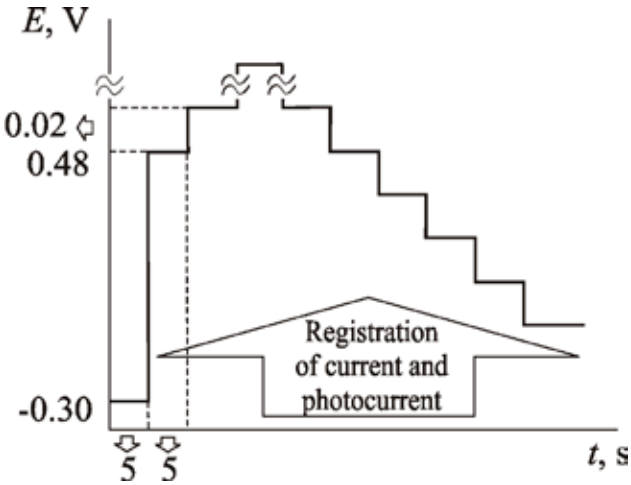


**Fig. 1.** Scheme of the potential step change in photoelectrochemical measurements

**Table 1.** The regime of pulse irradiation of oxide films on Ag–Pd alloys

| LED wavelength | Irradiation power | Photon flux density | Pulse duration | Pulse frequency |
|---|---|---|---|---|
| 470 nm | 0.1 mW/cm$^2$ | 1.18·10$^{14}$ photon/(s·cm$^2$) | 1000 ms | 5 Hz |

PhotoEdition potentiostat, manufactured in the laboratory of renewable energy sources of manufactured at the Laboratory of Renewable Energy Sources of Saint Petersburg National research Academic University of the Russian Academy of Sciences.

## 3. Results and discussion

### *3.1. Determination of the elemental and phase composition of alloys of the Ag-Pd system*

According to the results of energy dispersive X-ray analysis of the obtained alloys, the palladium concentration was consistent with the calculated until it did not exceed 20 at. % (Table 2). On an alloy with a calculated palladium concentration of 30 at. % much lower $X_{Pd}$ values have been experimentally determined. Probably such significant differences were due to the phase inhomogeneity of this sample.

According to X-ray diffractometry data, alloys with a palladium concentration of up to 20 at. % are characterized by the presence of only the alpha phase of the Ag(Pd) solid solution [37]. Similar results were obtained in [34, 35]. On the alloy with a calculated palladium concentration of 30 at. % in addition to the alpha phase Ag(Pd), a palladium phase was detected (Fig. 2). It can be assumed that an accumulation of the palladium phase occurs in the surface zone of the obtained alloys. A similar segregation of palladium as an electropositive component of the alloy was revealed in [38, 39]. Despite the deviation from homogeneity, this alloy was considered in the study of the photoelectrochemical activity of the anodic oxide films formed on it.

### *3.2. Cyclic voltammetry of alloys of the Ag–Pd system*

The voltammograms obtained in a deaerated 0.1 M KOH solution for all the studied alloys had similar shape (Fig. 3). On the anodic branch of the voltammogram, the current remained practically zero until the potential exceeded 0.42-0.52 V. A further increase in the potential led to an increase in the current.

On alloys with a palladium concentration of $X_{Pd}$ = 5–15 at. % the maximum current A1 was recorded, the potential of which $E_{A1}$ increased with increase in $X_{Pd}$ (Table 3). On pure silver, the potential of A1 maximum was 0.56 V [21]. On alloys with $X_{Pd}$ = 20 and 30 at. % a clear A1 maximum was not recorded, therefore the range of potentials for obtaining the anodic branch of

**Table 2.** Calculated and experimental composition, parameters of cycle voltammetry of Ag–Pd alloys, current efficiency of oxide formation processes and oxides thickness

| $\frac{X_{Pd}, \text{at.}\%}{X_{Ag}, \text{at.}\%}$ (calculated) | $\frac{5}{95}$ | $\frac{10}{90}$ | $\frac{15}{85}$ | $\frac{20}{80}$ | $\frac{30}{70}$ |
|---|---|---|---|---|---|
| $\frac{X_{Pd}, \text{at.}\%}{X_{Ag}, \text{at.}\%}$ (experimental) | $\frac{5.01\pm0.01}{94.99\pm1.59}$ | $\frac{9.81\pm0.03}{90.19\pm1.52}$ | $\frac{15.67\pm0.05}{84.33\pm1.23}$ | $\frac{20.51\pm0.08}{79.50\pm1.02}$ | $\frac{23.05\pm0.71}{76.95\pm2.30}$ |
| $E_{A1}$, V | 0.60 | 0.65 | 0.68 | 0.72 | 0.76 |
| $q_a$, mC/cm$^2$ | 59.5 | 53.2 | 58.6 | 77.0 | 45.8 |
| $q_{C1}$, mC /**c**m$^2$ | 49.2 | 34.0 | 37.4 | 33.9 | 14.5 |
| $q_{C2}$, mC /**c**m$^2$ | – | – | – | 16.4 | 10.3 |
| $q_{C3}$, mC /**c**m$^2$ | 8.0 | 13.4 | 16.4 | 23.4 | 13.1 |
| η($Ag_2O$), % | 83 | 64 | 64 | 44 | 32 |
| η(AgO), % | – | – | – | 21 | 22 |
| η(PdO), % | 13 | 25 | 28 | 30 | 29 |
| $L$($Ag_2O$), nm | 83 | 57 | 63 | 57 | 24 |
| $L$(AgO), nm | – | – | – | 14 | 17 |
| $L$(PdO), nm | 6 | 10 | 13 | 18 | 10 |

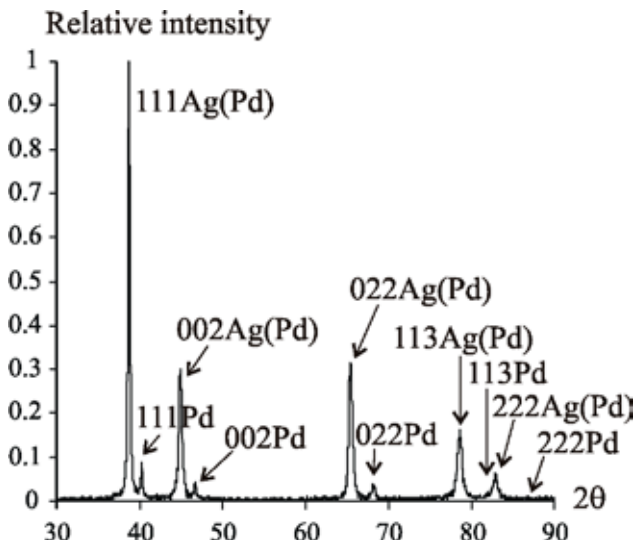


**Fig. 2.** X-ray diffraction patterns of the alloy with calculated palladium concentration of 30 at.%

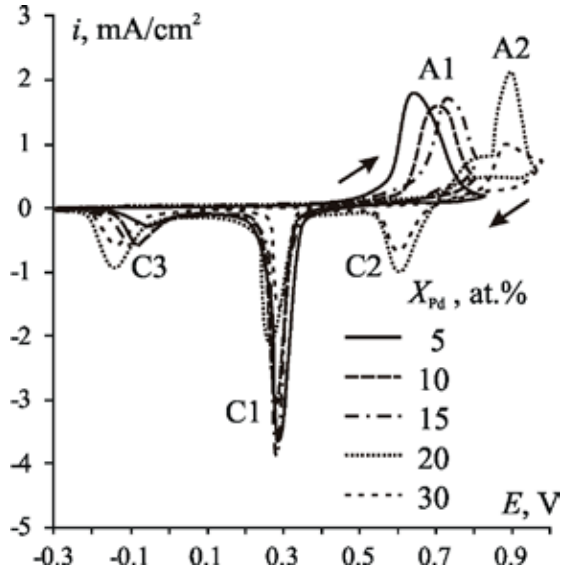


**Fig. 3.** Cycle voltammograms of Ag–Pd alloys in 0.1 M KOH at the potential scan rate of 5 mV/s

voltammograms was expanded. As a result, it was possible to observe a small step instead of the A1 peak, followed by a current A2 maximum, the potential of which was 0.9 V and did not depend on the palladium concentration in the alloy. The current density at the A1 and A2 maxima decreased with increasing palladium concentration, respectively, with decreasing silver concentration in the alloy.

Several maxima were recorded on the cathodic branch of the cyclic voltammogram depending on the palladium concentration and the direction of potential scan. Thus, on alloys with a palladium concentration from 5 to 15 at. % two maxima of the cathode current were registered, and on alloys with a palladium concentration of 20 and 30 at. % – three maxima were revealed (Fig. 3). The potentials of the C1 and C2 maxima are almost do not depend on the concentration of palladium in the alloy, and the current densities in them decrease with increasing $X_{Pd}$. The maximum cathode current C3 was recorded only on alloys, while it is absent on pure silver. Its potential decreased from approximately –0.05 to –0.14 V with increasing $X_{Pd}$ from 5 up to 30 at. %, and the amplitude generally increased.

Thermodynamic analysis and literature data can be used for the determination of the nature of the peaks. Thermodynamic analysis showed that both components of the investigated alloys were prone to oxide formation in the studied potential range. For the processes of formation of Ag(I) and Ag(II) oxides:

$$2Ag + 2OH^- = Ag_2O + H_2O + 2e^-,$$

$$Ag_2O + 2OH^- = 2AgO + H_2O + 2e^-$$

the equilibrium potentials in a 0.1 M KOH solution were $E^{eq}_{Ag2O/Ag} = 0.410$ V and $E^{eq}_{AgO/Ag2O} = 0.672$ V. In addition to the composition of the solution, the equilibrium potential depends on the composition of the electrode, namely, on the activity of silver. The less silver in the alloy, the higher the equilibrium potential for the formation of Ag(I) oxide.

Literature data [35, 40] and the experimentally observed increase of the potentials of peak A1 with increasing palladium concentration indicated that this peak corresponds to the formation of Ag(I) oxide. The AgO oxide was formed on a sublayer of Ag(I) oxide, and therefore the equilibrium potential of its formation did not depend on the composition of the alloy, which was observed experimentally for the A2 peak.

Subsequent cathodic reduction confirmed these assumptions. Thus, if on alloys with a relatively low concentration of palladium (5–15 at. %) only one A1 maximum was observed on the anode branch, then two current maxima were recorded on the cathode branch (C1 and C3). For alloys with higher palladium concentrations (20 and 30 at. %) three current maxima were

recorded on the cathode branch (C1, C2, and C3). Since the maximum of the cathodic current C3 was not recorded on pure silver, probably it was associated with the reduction of oxidized forms of palladium formed in the anodic period of obtaining voltammograms on the alloys. A similar interpretation of this current maximum was given in [35].

For processes of formation of Pd(II) oxide or hydroxide:

$Pd+2OH^- = PdO + H_2O+2e^-$,

$Pd+2OH^- = Pd(OH)_2 + 2e^-$

difference between equilibrium potentials in 0.1 M KOH solution was small: $E^{eq}_{Pd(OH)2/Pd} = 0.136$ V and $E^{eq}_{PdO/Pd} = 0.089$ V. Thus, the equilibrium potentials for the formation of palladium oxide or hydroxide were lower than the equilibrium potential for the formation of silver oxide. However, the maximum current associated with the formation of palladium oxide or hydroxide was not recorded in the voltammograms (Fig. 3). This situation is typical for the anodic formation of palladium oxide on alloys with a relatively low palladium content [41]. Thus, it is impossible to determine the formation of palladium oxide from the shape of the anodic voltammogram. At the same time, the maximum current C3 was clearly visible on the cathode branch at potentials lower than the potential of the maximum current characterizing the reduction of silver oxides C1 and C2 (Fig. 3). The fact that the amplitude of the C3 peak increased with increasing palladium concentration confirmed its nature associated with the reduction of palladium oxide or hydroxide. For definiteness, we will assume that the oxidized form of palladium is the oxide. The area under the C1 peak of the reduction of silver (I) oxide was much larger than the area under the reduction peak of palladium oxide (Fig. 3). Consequently, the main oxidation product of the studied alloys was Ag(I) oxide.

Density of cathode charges $q_{C1}$, $q_{C2}$, and $q_{C3}$ was calculated as the area under C1, C2 and C3 peaks, characterizing the reduction of $Ag_2O$, AgO, and PdO oxides (Fig. 3). The charge $q_{C1}$, characterizing the reduction of Ag(I) oxide, decreased from 49.2 to 14.5 mC/cm$^2$ when $X_{Pd}$ increased from 5 to 30 at. % (Table 2). The charge $q_{C3}$, characterizing the reduction of palladium oxide, increased from 8.0 to 23.4 mC/cm$^2$ when $X_{Pd}$ increased from 5 to 20 at.%, but decreased again during the transition to $X_{Pd}$ = 30 at. %. On the cathode branch of voltammograms of alloys with $X_{Pd}$ = 20 and 30 at. %, C2 maximum, corresponding to the reduction of AgO oxide also appeared. Calculation of the area under this maximum led to $q_{C2}$ values equal to 6.4 and 10.3 mC/cm$^2$ for alloys with a palladium concentration of 20 and 30 at. % respectively.

The current efficiency $\eta(Ag_2O)$, $\eta(AgO)$ and $\eta(PdO)$ was defined as the ratio of cathodic charges $q_{C1}$, $q_{C2}$ and $q_{C3}$ to the total anode charge $q_a$, accumulated during the anodic period of voltammetry of alloys. For each of the oxides, the current efficiency values were less than 100%. When the palladium concentration in the alloy increased from 5 to 30 at. % for Ag(I) oxide, the current efficiency decreased from 83 to 32% (Table 2). For palladium oxide, on the contrary, the current efficiency increased from 13 to 29%. For the AgO oxide, formed on alloys with palladium concentrations of 20 and 30 at.%, the current efficiency was 21 and 22%, respectively. The current efficiency of oxide formation $\eta(Ag_2O) + \eta(AgO) + \eta(PdO)$ also was less than 100%, which indicated a possible contribution from the processes of anodic formation of soluble silver oxidation products. A similar pattern was observed for pure silver [19–21].

Based on the magnitude of the cathode charges, the thickness of the oxides formed during the anodic period of obtaining voltamograms was calculated using Faraday's law. It should be noted that this calculation represents approximate estimation. It was performed under the assumption of uniform distribution of one of the formed oxides over the electrode area. For Ag(I) oxide, the estimated thickness $L(Ag_2O)$ decreased from 83 nm on an alloy with $X_{Pd}$ = 5 at. % up to 24 nm on alloy with $X_{Pd}$ = 30 at. %. The estimated thickness of palladium oxide $L(Ag_2O)$ increased from 6 nm on an alloy with $X_{Pd}$ = 5 at. % up to 18 nm on an alloy with $X_{Pd}$ = 20 at. %. A decrease in thickness was observed on the alloy with $X_{Pd}$ = 30 at. % , the decrease could be due to the impairment of the homogeneity of the structure of this alloy. The thickness of AgO oxide $L(Ag_2O)$, formed on alloys with $X_{Pd}$ = 20 and 30 at. %, was 14 and 17 nm, respectively (Table 2).

The visualization of the structure of the oxide film formed in the potentiodynamic polarization regime is quite difficult. It can be assumed that as the potential increased, the first was formed palladium oxide with an island structure. A further increase in potential led to the formation of Ag(I) oxide in areas free of palladium oxide. Due to the growth and fusion of nuclei, the Ag(I) oxide layer can cover the palladium oxide. The formation of a mixed oxide phase cannot be ruled out.

### 3.3. Photoelectrochemical activity of silver oxide

In preliminary experiments, with a stepwise increase in potential from $E_c$ with a step of 20 mV and a duration of each step of 5 min, it was revealed that the photocurrent was not recorded on the alloys until the potential reached 0.48 V. This finding indicates that during this time photosensitive oxide film did not form in an amount sufficient to exhibit photoelectrochemical activity. According to estimated calculations using the obtained current output (Table 2) the thickness of the Ag(I) oxide formed at the moment the potential reached 0.48 V did not exceed 4 nm. It should be noted that the equilibrium values for the formation of palladium oxide were already significantly exceeded. The thickness of the palladium oxide formed at this point cannot be estimated. However, it was obvious, that even if some palladium oxide was formed, its photoelectrochemical activity had not yet manifested itself.

At potentials of 0.48 V and higher, an anodic photocurrent started to be recorded on silver and alloys (Fig. 4), indicating the n-type conductivity of the formed oxide film. The lower the concentration of silver in the alloy, the higher the potential at which photocurrent starts to be generated. With increasing potential in the anodic direction to values exceeding the potential of A1 maximum, photocurrent increased, reaching maximum values $i_{ph}^{max}$(A) at potentials $E_{ph}^{max}$(A) (Table 3). Values of $E_{ph}^{max}$(A) were higher than $E_{A1}$ on voltammograms.

After changing the direction of potential scan to the cathode, the photocurrent continued to increase. This can be explained by the continuation of the formation process and thickening of the oxide film, since the polarization currents remained anodic. The exception was silver and an alloy with an atomic fraction of palladium of 5 at. %, where after changing the direction of potential scan, the photocurrent immediately started to decrease. On alloys with higher palladium content, the photocurrent started to decrease at lower potentials.

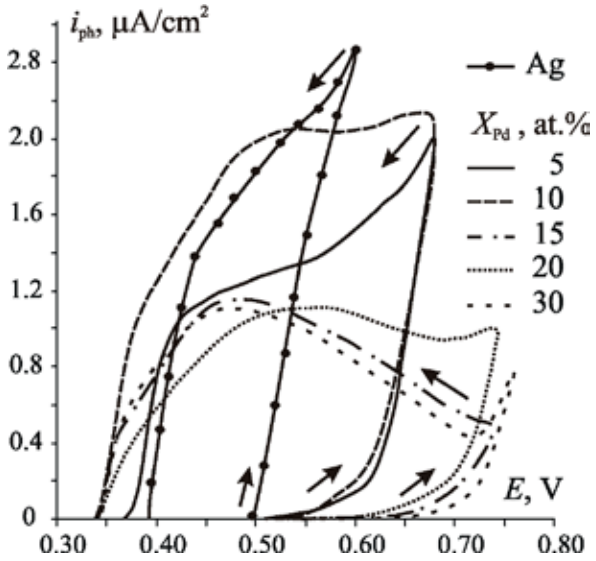


**Fig. 4.** Photocurrent during the anodic and cathodic direction of the potential change of silver and Ag–Pd alloys in 0.1 KOH

**Table 3.** Parameters of photoelectrochemical activity

| $X_{Pd,}$ at.% | 0 | 5 | 10 | 15 | 20 | 30 |
|---|---|---|---|---|---|---|
| Anodic direction of potential scanning | | | | | | |
| $E_{ph}^{max}$(A), V | 0.60 | 0.68 | 0.68 | 0.74 | 0.74 | 0.76 |
| $i_{ph}^{max}$(A), μA/cm² | 2.89 | 1.99 | 1.94 | 0.90 | 0.47 | 0.78 |
| IPCE$^{max}$(A), % | 7.62 | 5.25 | 5.12 | 2.37 | 1.24 | 2.06 |
| Cathodic direction of potential scanning | | | | | | |
| $E_{ph}^{max}$(C), V | 0.60 | 0.68 | 0.66 | 0.56 | 0.48 | 0.46 |
| $i_{ph}^{max}$(C), μA/cm² | 2.89 | 1.99 | 2.12 | 1.11 | 1.16 | 1.10 |
| IPCE$^{max}$(C), % | 7.62 | 5.25 | 5.59 | 2.93 | 3.06 | 2.90 |

The photoelectrochemical activity of the oxide on silver disappeared at 0.38 V, and on alloys, at approximately the same potential values, about 0.3 V, most probably corresponding to the complete reduction of silver oxide. Indeed, the C1 maximum, corresponding to the reduction of Ag(I) oxide, was observed in cyclic voltammograms at potentials of about 0.3 V. The C1 maximum on silver and the alloy with $X_{Pd}$ = 5 at. % was slightly higher than on other alloys. Since the reduction potentials of palladium oxide have not yet been achieved, its existence on the surface of alloys cannot be ruled out. However, photocurrent was no longer generated, e.g. palladium oxide was not a photoelectrochemically active material under experimental conditions. Nevertheless, the presence of palladium in the alloy made a certain contribution to the photoelectrochemical activity of anodicly formed oxide films.

Thus, with increasing palladium, concentration potential $E_{ph}^{max}$(A), at which the maximum photocurrent was recorded in the anodic direction, also increased, and the maximum photocurrent density $i_{ph}^{max}$(A) decreased (Table 3). The potential $E_{ph}^{max}$(C), at which the maximum photocurrent was recorded $i_{ph}^{max}$(C), decreased with increasing palladium concentration after changing the direction of potential scan from anodic to cathodic. The alloy with an atomic fraction of palladium of 10 at. % was characterized by the highest photoelectrochemical activity. On this alloy, as the potential swept to the cathode, the highest photocurrent density $i_{ph}^{max}$(C) was recorded at $E_{ph}^{max}$(C) = 0.66 V. This value was close to the anodic peak potential $E_{A1}$ on the voltammogram (Table 2). In the oxide film on silver, it was possible to register higher photocurrent values of 2.89 μA/cm$^2$, with incidental proton-to-electron conversion efficiency of 7.62%.

The maximum incidental proton-to-electron conversion efficiency, calculated based on the maximum values of photocurrent density, did not exceed 6% for all alloys. Changes of IPCE$^{max}$ depending on the palladium concentration in the alloy, correlated with changes in the maximum photocurrent. When the potential swept to the anode, photoelectrocatalytic activity decreased with increasing palladium concentration in the alloy. When the potential swept to the cathode, the maximum photoelectrocatalytic activity was recorded in an oxide film formed anodically on an alloy with an atomic fraction of palladium of 10 at. %.

## 4. Conclusions

During the anodic oxidation of silver and alloys of the Ag–Pd system in an alkaline deaerated solution of 0.1 M KOH in the potential range up to 0.76 V (SHE), silver oxide (I) was predominantly formed. The current efficiency of its formation decreased from 83 to 32% with an increase in the calculated palladium concentration from 5 to 30 at. %. The formation of palladium oxide with a current efficiency of 6–18%, depending on the composition of the alloy, is also possible. The potential range of photoelectrochemical activity of formed anodicly oxide films averaged from 0.35 to 0.76 V (st.h.e.). In the indicated potential range on silver and all alloys, under pulsed illumination, a positive photocurrent was generated, which indicated the predominance of donor structural defects in the forming oxide film. An increase in palladium concentration led to an expansion of the potential regions of photoelectrochemical activity of oxide films formed anodically on alloys of the Ag–Pd system. During the anodic potentiodynamic formation of an oxide film on alloys, the potential at which the maximum photocurrent was recorded increased with increasing palladium concentration, while the maximum photocurrent and the incidental proton-to-electron conversion efficiency generally decreased. During the cathodic potentiodynamic reduction of the formed oxide films, it was possible to record even higher photocurrents than during their anodic formation. The highest photoelectrochemical activity, characterized by the photocurrent density of 2.89 μA/cm$^2$ and the incidental proton-to-electron conversion efficiency of 7.62%, was observed in an oxide film formed anodically on silver. Comparable values (2.12 μA/cm$^2$ and 5.59%) were registered in an oxide film of an alloy with an atomic fraction of palladium of 10 at. %, during its potentiodynamic reduction.

## Contribution of the authors

The authors contributed equally to this article.

## Conflict of interests

The authors declare that they have no known competing financial interests or personal

relationships that could have influenced the work reported in this paper.

## References

1. Septina W., Ikeda Sh., Khan M. A., ... Peter L. M. Potentiostatic electrodeposition of cuprous oxide thin films for photovoltaic applications. *Electrochimica Acta*. 2011;56(13): 4882–4888. https://doi.org/10.1016/j.electacta.2011.02.075

2. Strehblow H. H., Milosev I. Electrochemical behavior of Cu-xZn alloys in borate buffer solution at pH 9.2. *Journal of the Electrochemical Society*. 2003;150(11): B517–B524. https://doi.org/10.1149/1.1615997

3. Singh N., Choudhary S., Upadhyay S., Satsangi V. R., Dass S., Shrivastav R. Nanocrystalline $Zn_{1-x}Ag_xO_y$ thin films evolved through electrodeposition for photoelectrochemical splitting of water. *Journal of Solid State Electrochemistry*. 2014;18(2): 523–533. https://doi.org/10.1007/s10008-013-2285-y

4. Zhu S., Wang D. Photocatalysis: basic principles, diverse forms of implementations and emerging scientific opportunities. *Advanced Energy Materials*. 2017;7(23): 1700841. https://doi.org/10.1002/aenm.201700841

5. Navarro R. M., Álvarez Galván M. C., del Valle F., Villoria de la Mano J. A., Fierro J. L. G. Water splitting on semiconductor catalysts under visible-light irradiation. *ChemSusChem*. 2009;2(6): 471–485. https://doi.org/10.1002/cssc.200900018

6. Kozlova E. A., Parmon V. N. Heterogeneous semiconductor photocatalysts for hydrogen production from aqueous solutions of electron donors. *Russian Chemical Reviews*. 2017;86(9): 870. https://doi.org/10.1070/rcr4739

7. Ge J., Zhang Y., Heo Y.-J., Park S.-J. Advanced design and synthesis of composite photocatalysts for the remediation of wastewater: A review. *Catalysts*. 2019;9(2): 122. https://doi.org/10.3390/catal9020122

8. Sadovnikov S. I., Kozlova E. A., Gerasimov E. Yu., Rempel A. A., Gusev A. I. Enhanced photocatalytic hydrogen evolution from aqueous solutions on $Ag_2S$/Ag heteronanostructure. *International Journal of Hydrogen Energy*. 2017;42(40): 25258–25266. https://doi.org/10.1016/j.ijhydene.2017.08.145

9. Markovskaya D. V., Gribov E. N., Kozlova E. A., Kozlov D. V., Parmon V. N. Modification of sulfide-based photocatalyst with zinc-and nickel-containing compounds: Correlation between photocatalytic activity and photoelectrochemical parameters. *Renewable Energy*. 2020;151: 286–294. https://doi.org/10.1016/j.renene.2019.11.030

10. He H., Liao A., Guo W., Luo W., Zhou Y., Zou Z. State-of-the-art progress in the use of ternary metal oxides as photoelectrode materials for water splitting and organic synthesis. *Nano Today*. 2019;28: 100763. https://doi.org/10.1016/j.nantod.2019.100763

11. Mehdi H. E., Hantehzadeh M. R., Valedbagi Sh. Physical properties of silver oxide thin film prepared by DC magnetron sputtering: effect of oxygen partial pressure during growth. *Journal of Fusion Energy*. 2013;32(1): 28–33. https://doi.org/10.1007/s10894-012-9509-5

12. Gao X.-Y., Wang S.-Y., Li J., ... Chen L.-Y. Study of structure and optical properties of silver oxide films by ellipsometry, XRD and XPS methods. *Thin Solid Films*. 2004;455-456: 438–442. https://doi.org/10.1016/j.tsf.2003.11.242

13. Barik U. K., Srinivasan S., Nagendra C. L., Subrahmanyam A. Electrical and optical properties of reactive DC magnetron sputtered silver oxide thin films: role of oxygen. *Thin Solid Films*. 2003;429(1-2): 129–134. https://doi.org/10.1016/S0040-6090(03)00064-6

14. Ida Y., Watase S., Shinagawa T., ... Izaki M. Direct electrodeposition of 1.46 eV band gap silver (I) oxide semiconductor films by electrogenerated acid. *Chemistry of Materials*. 2008;20(4): 1254–1256. https://doi.org/10.1021/cm702865r

15. Ferretti A. M., Ponti A., Molteni G. Silver(I) oxide nanoparticles as a catalyst in the azide–alkyne cycloaddition. *Tetrahedron Letters*. 2015;56(42): 5727–5730. https://doi.org/10.1016/j.tetlet.2015.08.083

16. Wei J., Lei Y., Jia H., Cheng J., Hou H., Zheng Z. Controlled in situ fabrication of $Ag_2O$/AgO thin films by a dry chemical route at room temperature for hybrid solar cells. *Dalton Transactions*. 2014;43(29): 11333–11338. https://doi.org/10.1039/c4dt00827h

17. Wang W., Zhao Q., Dong J., Li J. A novel silver oxides oxygen evolving catalyst for water splitting. *International Journal of Hydrogen Energy*. 2011;36(13): 7374–7380. https://doi.org/10.1016/j.ijhydene.2011.03.096

18. Yin Z., Liangxu X., Cao S., Xiao Y. Ag/$Ag_2O$ confined visible-light driven catalyst for highly efficient selective hydrogenation of nitroarenes in pure water medium at room temperature. *Chemical Engineering Journal*. 2020;394: 125036. https://doi.org/10.1016/j.cej.2020.125036

19. Vvedenskii A. V., Grushevskaya S. N., Kudryashov D. A., Ganzha S. V. *Thin oxide films on metals and alloys: kinetics of anodic formation and photoelectrochemical properties*[*]. Voronezh: Publishing and printing center «Nauchnaya kniga»; 2016. 296 p. (In Russ.)

20. Vvedenskii A., Grushevskaya S., Kudryashov D., Kuznetsova T. Kinetic peculiarities of anodic dissolution of silver and Ag-Au alloys under the conditions of oxide formation. *Corrosion Science*.

2007;49(12): 4523–4541. https://doi.org/10.1016/j.corsci.2007.03.046

21. Vvedenskii A., Grushevskaya S., Kudryashov D., Ganzha S. The influence of the conditions of the anodic formation and the thickness of Ag (I) oxide nanofilm on its semiconductor properties. *Journal of Solid State Electrochemical*. 2010;14(8): 1401–1413. https://doi.org/10.1007/s10008-009-0952-9

22. Belyanskaya I. A., Taran A. I., Grushevskaya S. N., Vvedenskii A. V. Anodic formation and characteristics of silver oxides on alloys of Ag-Zn system. *Proceedings of Voronezh State University. Series: Chemistry. Biology. Pharmacy*. 2020;(3): 5–13. (In Russ., abstract in Eng.). Available at: https://elibrary.ru/title_about_new.asp?id=9907

23. Bocharnikova M. Yu., Murtazin M. M., Grushevskaya S. N., Kozaderov O. A., Vvedensky A. V. Anodic formation and properties of nanoscale oxide layers on silver–zinc alloys with different concentrations of nonequilibrium vacancies. *Journal of Solid State Electrochemistry*. 2022;26(8): 1637–1644. https://doi.org/10.1007/s10008-022-05204-z

24. McCarthy S., Braddock D. C., Wilton-Ely J. D. E. T. Strategies for sustainable palladium catalysis. *Coordination Chemistry Reviews*. 2021;442: 213925. https://doi.org/10.1016/j.ccr.2021.213925

25. Li Z., Meng X. Recent development on palladium enhanced photocatalytic activity: A review. *Journal of Alloys and Compounds*. 2020;830: 154669. https://doi.org/10.1016/j.jallcom.2020.154669

26. Ryabtsev S. V., Ievlev V. M., Samoylov A. M., Kuschev S. B., Soldatenko S. A. Microstructure and electrical properties of palladium oxide thin films for oxidizing gases detection. *Thin Solid Films*. 2017;636; 751–759. https://doi.org/10.1016/j.tsf.2017.04.009

27. Chiang Y.-J., Pan F.-M. PdO nanoflake thin films for CO gas sensing at low temperatures. *The Journal of Physical Chemistry C*. 2013;117: 15593–15601. https://doi.org/10.1021/jp402074w

28. Arora K., Srivastava S., Solanki P. R., Puri N. K. Electrochemical hydrogen gas sensing employing palladium oxide/reduced graphene oxide (PdO-rGO) nanocomposites. *IEEE Sensors Journal*. 2019;19(18): 8262–8271. https://doi.org/10.1109/JSEN.2019.2918360

29. Wang J., Fan X., Liu B., Li C., Bai J. $Eu_xO_y$-PdO catalyst concerted efficiently catalyzes Suzuki-Miyaura coupling reaction. *Materials Chemistry and Physics*. 2020;252: 123227. https://doi.org/10.1016/j.matchemphys.2020.123227

30. Mahara Y., Murata K., Ueda K., Ohyama J., Kato K., Satsuma A. Time resolved in situ DXAFS revealing highly active species of PdO nanoparticle catalyst for $CH_4$ oxidation. *ChemCatChem*. 2018;10: 3384–3387. https://doi.org/10.1002/cctc.201800573

31. Rao F., Zhu G., Wang M., ... Hojamberdiev M. Constructing the Pd/PdO/β-$Bi_2O_3$ microspheres with enhanced photocatalytic activity for Bisphenol A degradation and NO removal. *Journal of Chemical Technology & Biotechnology*. 2020;95(3): 862–874. https://doi.org/10.1002/jctb.6276

32. Nguyen T. D., Cao V. D., Nong L. X., ... Vo D.-V. N. High photocatalytic performance of Pd/PdO-supported $BiVO_4$ nanoparticles for Rhodamine B degradation under visible LED light irradiation. *ChemistrySelect*. 2019;4(20): 6048–6054. https://doi.org/10.1002/slct.201901295

33. Zahra T., Ahmad K. S., Thomas A. G., ... Sohail M. Phyto-inspired and scalable approach for the synthesis of PdO–2$Mn_2O_3$: A nano-material for application in water splitting electro-catalysis. *RSC Advances*. 2020;10(50): 29961–29974. https://doi.org/10.1039/D0RA04571C

34. Zeledón Z. J. A., Stevens M. B., Gunasooriya G. T. K. K., ... Jaramillo T. F. Tuning the electronic structure of Ag–Pd alloys to enhance performance for alkaline oxygen reduction. *Nat Commun*. 2021;12: 620. https://doi.org/10.1038/s41467-021-20923-z

35. Slanac D. A., Hardin W. G., Johnston K. P., Stevenson K. J. Atomic ensemble and electronic effects in Ag-Rich AgPd nanoalloy catalysts for oxygen reduction in alkaline media. *Journal of the American Chemical Society*. 2012;134(23): 9812–9819. https://doi.org/10.1021/ja303580b

36. Grinberg V. A., Emec V. V., Majorova N. A., ... Codikov M. V. Photoelectrochemical activity of nanosized titania, doped with bismuth and lead, in visible light region. *Protection of Metals and Physical Chemistry of Surfaces*. 2019;55(1): 55–64. https://doi.org/10.1134/S0044185619010121

37. Belyanskaya I. A., Bocharnikova M. Yu., Grushevskaya S. N., Kozaderov O. A., Vvedenskii A. V., Kannykin S. V. Anodic formation and photoelectrochemical characteristics of Ag(I) oxide on the Ag–Pd-system alloys. *Russian Journal of Electrochemistry*. 2024;60(6): 468–477, in press.

38. Wouda P. T., Schmid M., Nieuwenhuys B. E., Varga P. STM study of the (111) and (100) surfaces of PdAg. *Surface Science*. 1998;417(2-3): 292–300. https://doi.org/10.1016/S0039-6028(98)00673-6

39. Zhao M., Brouwer J. C., Sloof W. G., Bottger A. J. Surface segregation of Pd-Cu alloy in various gas atmospheres. *International Journal of*

*Hydrogen Energy*. 2020;45: 21567e21572. https://doi.org/10.1016/j.ijhydene.2020.05.268

40. Hecht D., Borthen P., Strehblow H. -H. In situ examination of anodic silver oxide films by EXAFS in the reflection mode. *Journal of Electroanalytical Chemistry*. 1995;381: 113–121. https://doi.org/10.1016/0022-0728(94)03611-6

41. Bolzan A. E. Phenomenological aspects related to the electrochemical behaviour of smooth palladium electrodes in alkaline solutions. *Journal of Electroanalytical Chemistry*. 1995;380: 127–138. https://doi.org/10.1016/0022-0728(94)03627-F

**Translated by author of the article*

**Information about the authors**

*Irina A. Belyanskaya,* postgraduate student, Voronezh State University (Voronezh, Russian Federation).

belyanskaya_98@mail.ru

*Maria Y. Bocharnikova,* Engineer at the Department of Physical Chemistry, Voronezh State University (Voronezh, Russian Federation).

https://orcid.org/0009-0003-5420-6848

nesterovamarija18@gmail.com

*Maksim M. Murtazin,* Cand. Sci. (Chem.), Junior Researcher at LLC "NPO Membranes" (Voronezh, Russian Federation).

https://orcid.org/0009-0005-9574-4057

murtazin@chem.vsu.ru

*Svetlana N. Grushevskaya,* Cand. Sci. (Chem.), Associate Professor at the Department of Physical Chemistry, Voronezh State University (Voronezh, Russian Federation).

https://orcid.org/0000-0002-7083-1438

sg@chem.vsu.ru

*Oleg A. Kozaderov,* Dr. Sci. (Chem.), Senior Researcher, Laboratory of Organic Additives for the Processes of Chemical and Electrochemical Deposition of Metals and Alloys Used in the Electronics Industry, Voronezh State University (Voronezh, Russian Federation).

https://orcid.org/0000-0002-0249-9517

ok@chem.vsu.ru

*Alexander V. Vvedenskii,* Dr. Sci. (Chem.), Professor at the Department of Physical Chemistry, Voronezh State University (Voronezh, Russian Federation).

https://orcid.org/0000-0003-2210-5543

alvved@chem.vsu.ru

*Received 11.09.2023; approved after reviewing 02.10.2023; accepted for publication 15.11.2023; published online 25.06.2024.*

*Translated by Valentina Mittova*